Int. J. Electrochem. Sci., 16 **(2021)** Article Number: 211045, doi: 10.20964/2021.10.08

International Journal of
ELECTROCHEMICAL
SCIENCE
www.electrochemsci.org

Electro-oxidation of Methanol, Ethanol and Ethylene Glycol over Pt/TiO_2-C and PtSn/TiO_2-C Anodic Catalysts

Chih-Wei Tang[1,], Chiu-Hung Liu[2], Chih-Chia Wang[3,4] and Chen-Bin Wang[3,4,*]*

[1] Department of General Education, Army Academy ROC, Taoyuan, 32092, Taiwan, ROC
[2] Graduate School of National Defense Science, Chung Cheng Institute of Technology, National Defense University, Taoyuan, Taiwan, ROC
[3] Department of Chemical and Materials Engineering, Chung Cheng Institute of Technology, National Defense University, Taoyuan, Taiwan, ROC
[4] System Engineering and Technology Program, National Chiao Tung University, Hsinchu, Taiwan, ROC
[*]E-mail: cwtang@aaroc.edu.tw (C.W. Tang) and chenbinwang@gmail.com (C.B. Wang).

Received: 31 May 2021 / *Accepted:* 29 July 2021 / *Published:* 10 September 2021

This study focused on the use of a modified Pt/C anodic catalyst with doping tin (Sn) and titania (TiO_2) to improve the efficiency and effective of direct alcohols (methanol, ethanol and ethylene glycol) fuel cells. Decorated the TiO_2 dopant on active carbon support (xTiO_2-C, x = 10, 20, 30, 40 weight percent) was completed by the impregnation method. Then, the series Pt/TiO_2-C and PtSn/TiO_2-C anodic catalysts were prepared by the formic acid reduction method using $PtCl_4$ and $SnCl_2{\cdot}2H_2O$ as platinum (Pt, 10 wt%) and tin (Sn, 10 wt%) precursors. The fabricated series anodic catalysts were painted on carbon paper as working electrodes. Evaluation of the catalytic activity for the electro-oxidation of alcohols on working electrodes was performed by cyclic voltammetry (CV) in 0.5 M H_2SO_4 and 1 M alcohol electrolytes at room temperature. The results showed that all the doped TiO_2 and Sn anodic catalysts present well-dispersed platinum with a diameter around 3 - 5 nm. In addition, the activity for electro-oxidation of alcohols was affected remarkably by the content of TiO_2 and Sn in the anodic catalysts. Among the prepared Pt/TiO_2-C and PtSn/TiO_2-C anodic catalysts, the 30 wt% TiO_2 catalyst exhibited the best catalytic performance. In comparison with the various alcohols, the the tendency of activity for the ethanol electro-oxidation was : ethanol > methanol > ethylene glycol.

Keywords: Pt/TiO_2-C; PtSn/TiO_2-C; Electro-oxidation of alcohol; Cyclic voltammetry.

1. INTRODUCTION

Research on fuel cell technology has attracted much attention in recent years [1-3]. Fuels such as small organic alcohol molecule, methanol (MeOH), ethanol (EtOH), and ethylene glycol (EG) are

easy to carry, high energy density, low toxicity, and easy converted from biomass, which play an important role in energy storage and conversion [4-8]. In order to reduce carbon dioxide emissions and establish a sustainable carbon cycle, the use of direct alcohol fuel cells can directly convert the chemical energy into electrical energy [9, 10]. Among them, electro-reforming of alcohol can be carried out under low temperature and atmospheric pressure [11], which is an energy-saving, low-cost and environmentally friendly technology. In order to effectively realize this energy conversion, it is necessary to select a suitable catalyst to accelerate the electro-catalytic process. Platinum-based catalysts are often used in the reactions of methanol and ethanol due to their high intrinsic activity and good chemical stability [12, 13]. However, the application of Pt-based catalysts in fuel cells is limited by factors such as the reaction intermediate CO, which is easy to poison the catalyst and expensive. These need to develop alternative materials to reduce costs and eliminate CO [14-17]. In order to inhibit the poison of anodic catalysts on the ethanol electro-oxidation, Simoes *et al* [14] confirmed that the PtSn bimetallic catalysts could mitigate the poisoning effect of CO.

The performance of platinum catalysts can be improved by adjusting the composition, electronic structure, and developing novel catalysts [15, 18], such as forming alloys or doping with other metal atoms or metal oxides. Combining the dual-function, electronic and overall effects of the composite materials can improve catalytic activity and stability [16, 17, 19]. An effective way to improve the electro-catalytic performance and stability of Pt-based catalysts is to disperse the Pt nanoparticles on promoters or conductive supports [20]. The promoters can not only support the Pt nanoparticles, but also enhanceed the catalytic performance [21, 22]. Compared with the conductive carrier, the promoter was more effective in improving the catalytic performance of Pt-based catalysts. For example, embedding CeO_2 particles in carbon nanofibers resulted in blocking the contact between Pt nanoparticles and CeO_2, which appreciably enhanced the catalytic performance and durability [23]. In acidic solutions, TiO_2 owned high catalytic performance and stability [24-26]. Javier et al. [25] fabricated a TiO_2/SBA-15 photocatalyst to effectively promote the oxidation of alcohol under ultraviolet irradiation. In the electro-oxidation of ethanol study, Brian et al. [26] affirmed the preferential activity of Pt/TiO_2 catalyst. Since there were not enough reports to continue to support these observation, based on the curiosity, we developped series Pt/TiO_2-C and Pt(Sn)/TiO_2-C anodic catalysts and applied on the alcohol fuels oxidation. To evaluate the efficiency and effectiveness on the electro-oxidation of methanol, ethanol and ethylene glycol by using cyclic voltammetry (CV) had been researched in this work.

2. EXPERIMENTAL

The xTiO_2-C supports (x = 10, 20, 30, 40 wt%) were fabricated by the impregnation method as described in the previous paper [27] using $Ti(OC_4H_9)_4$ (Merck) as titania precursor and active carbon (S.A. 240 $m^2 \cdot g^{-1}$, Cabot). After the xTiO_2 doped on active carbon, the obtained slurry was dried overnight at 110 °C. The series Pt/TiO_2-C and Pt(Sn)/TiO_2-C anodic catalysts were prepared by the formic acid reduction method as described elsewhere [27, 28] using $PtCl_4$ (Strem Chemicals) and $SnCl_2 \cdot 2H_2O$ (Acros Organics) as platinum (Pt, 10 wt%) and tin (Sn, 10 wt%) precursors. After Pt and PtSn deposition, the obtained slurry was dried overnight at 110 °C.

The surface area of series anodic catalysts was measured and calculated through the nitrogen physisorption and BET equation on a Quantachrome Autosorb-1 apparatus (at 77 K). The average size and distribution of the series anodic catalysts were observed by using a transmission electron microscope (TEM) with a JEM-2010 microscope (JEOL) under an acceleration voltage of 200 kV. The reduction property of series anodic catalysts was investigated with temperature programmed reduction (TPR) system (with a 30 $mL \cdot min^{-1}$ flow rate of 10% H_2 in N_2 stream at a rate of 7 $°C \cdot min^{-1}$) in the range of – 50 to 200 °C.

The electrochemical analyzer (CH Instruments 611C) instrument was chosen to measure the electrochemical capability using a three-electrode cell under 25 °C. Tuned inks of series Pt/TiO_2-C and $PtSn/TiO_2$-C anodic catalysts were painted on the central region of carbon paper (4 $mg \cdot cm^{-2}$) acted as a working electrode, also, both the Pt foil and saturated calomel electrode (SCE) were picked as the counter and reference electrodes. All electrode potentials referred to the SCE in the measurement of electrochemical capability. The cyclic voltammetry (CV) evaluation of methanol (MOR), ethanol (EOR) and ethylene glycol (EGOR) was carried out around – 0.2 to 1.0 V potential vs SCE under nitrogen environment. In the 0.5 M H_2SO_4 and 1 M methanol, ethanol or ethylene glycol electrolyte solution, the scan rate was controlled at 10 $mV \cdot s^{-1}$. Before each experiment, electrolyte solution was purged under nitrogen gas for 1 h. The electrochemical active surface (EAS) of Pt-based catalysts was evaluated by the area of hydrogen adsorption and desorption (– 0.15 to 0.25 V) on the CV in a 0.5 M H_2SO_4 blank solution under 25 °C with a scanning rate of 50 $mV \cdot s^{-1}$ according to the equation (1) [29].

$$EAS = Q_H / M_{Pt} \cdot Q_{Href} \quad (1)$$

Where Q_H was the average charge of H-atoms electro-adsorption and electro-desorption on the surface of Pt-based catalysts, M_{Pt} was the mass of loaded platinum, and Q_{Href} was the charge required for oxidation of monolayer adsorbed H-atoms on the catalyst surface (assuming 0.21 $mC \cdot cm^{-2}$ corresponds to the surface density of 1.3×10^{15} $atom \cdot cm^{-2}$) [30, 31]. The measurement of chronoamperometry was executed under 0.45 V with a scanning time of 3600 s in methanol, ethanol and ethylene glycol solution, respectively.

3. RESULTS AND DISCUSSION

3.1 Characterization of catalyst

Figure 1 shows the TEM images of series Pt/TiO_2-C (Fig. 1(a)) and $PtSn/TiO_2$-C (Fig. 1(b)) catalysts, and the corresponding particle size distribution histograms. From the analysis of TEM photographs, it is clear that the shape of the Pt particles is approximately spherical. Compare the particle size distribution of Pt/C and Pt/TiO_2-C catalysts, it found that the Pt/C catalyst is easy agglomeration and the average particle size of Pt is about 6.9 nm. In the study of oxidation of formaldehyde, Zhang et al [32] found that the doped TiO_2 could disperse effectively the Pt particle. Apparently, the addition of proper amount TiO_2 can improve the dispersion of active species and drops the Pt particles to 5.0 nm. Compare the particle size distribution of PtSn/C and $PtSn/TiO_2$-C catalysts, apparently, the active species can be well-dispersed via simultaneous addition of Sn and TiO_2 and further reduces the Pt

particles below 4.0 nm. The PtSn/30TiO_2-C catalyst is preferential well-dispersed among these anodic catalysts and the Pt particle size approaches 3.0 nm. The average particle size of series catalysts is listed in the 2nd column of Table 1.

Figure 2 displays the XRD patterns of series Pt/TiO_2-C (Fig. 2(a)) and PtSn/TiO_2-C (Fig. 2(b)) catalysts, and the N_2 adsorption/desorption isotherms of Pt/30TiO_2-C (Fig. 2(c)) and PtSn/30TiO_2-C (Fig. 2(d)) catalysts. Compare the profiles of Pt/C with Pt/TiO_2-C and PtSn/TiO_2-C catalysts, both position (2θ of 39.8°and 46.3° were ascribed to the (111) and (200) planes of Pt, 24º, 39º and 46º were ascribed to the (111), (220) and (311) planes of $PtSn_2$, respectively) and intensity of the main diffraction peaks are very similar, and only faint peaks of TiO_2 is observed. It can be affirmed that all catalysts display a face centered cubic (fcc) crystalline of platinum and the amorphous TiO_2 phase. Look earnestly, the diffraction peaks become broad and shift to lower angle as the addition of Sn and TiO_2, especially for the addition of Sn into the Pt appreciably reduces the particle size (d_{Pt}). It confirms that the doped Sn can intercalate into the Pt lattice to form $PtSn_2$ alloy as reported previously [33-36]. Choosing the prominent peak of (111) plane of Pt and using the Scherrer equation calculates the d_{Pt}, and attached to the figure. The calculated d_{Pt} matches to the true values from the TEM analysis. Also, the PtSn/30TiO_2-C catalyst shows the best dispersion among these anodic catalysts and the calculated d_{Pt} is 3.4 nm. The N_2 adsorption/desorption isotherms of Pt/30TiO_2-C (Fig. 2(c)) and PtSn/30TiO_2-C (Fig. 2(d)) displays the similar surface area for both catalysts. The surface area of series catalysts is listed in the 3rd column of Table 1. Apparently, the specific surface area of the catalyst decreases gradually with the increase of TiO_2.

In order to eliminate the interference of the chloride ion reduction, the 1st running of TPR samples is further oxidized at 100 ℃. Then, the 2nd running of TPR is recorded. Figure 3 exhibits the TPR profiles of series Pt/TiO_2-C (Fig. 3(a)) and PtSn/TiO_2-C (Fig. 3(b)) catalysts. Based on the reported of literatures [37, 38], two reduction signals can be distinguished at low temperature (T_{r1}: - 45 ~ - 5 °C) and high temperature (T_{r2}: 95 ~ 125 °C), and is listed in the last two columns of Table 1. The T_{r1} is the reduction of surface active oxides (Pt^sO_x and/or $PtSn_2{}^sO_x$, Pt^s and $PtSn_2{}^s$ assigned as the surface active species of Pt metal and $PtSn_2$ alloy), which is weak interaction between this species and support, so, it can be reduced at low temperature. While, the T_{r2} is the reduction of strong interaction between the PtO_x and/or $PtSn_2O_x$ species with support, so, it reduces at high temperature. Comparing the reduction behavior of a series of anodic catalysts, the T_r of highly dispersed $PtSn_2{}^sO_x$ is lower than the Pt^sO_x. In addition, the TiO_2-doped active carbon can effectively disperse the active species to reduce the T_r of the catalyst.

In addition to the surface area and particle size of catalysts can influence the electro-catalytic activity, the cyclic voltammetry (CV) can also be chosen to further measure the content of relative active site on the catalyst surface. Generally, the more contents of active sites possess better activity. In an acidic electrolyte, the average charge of the electro-adsorption and electro-desorption of hydrogen on the surface of anodic catalyst can be measured by the CV, and the EAS of the catalyst can be measured by the equation (1). The EAS of series anodic catalysts is listed in the 4th column of Table 1. According to the quantitative estimation of the current density in district of double-layer reduction, the EAS value of the series PtSn/TiO_2-C catalysts is about 1.3 and 5.4 times higher than those of the series Pt/TiO_2-C and Pt/C catalysts, respectively.

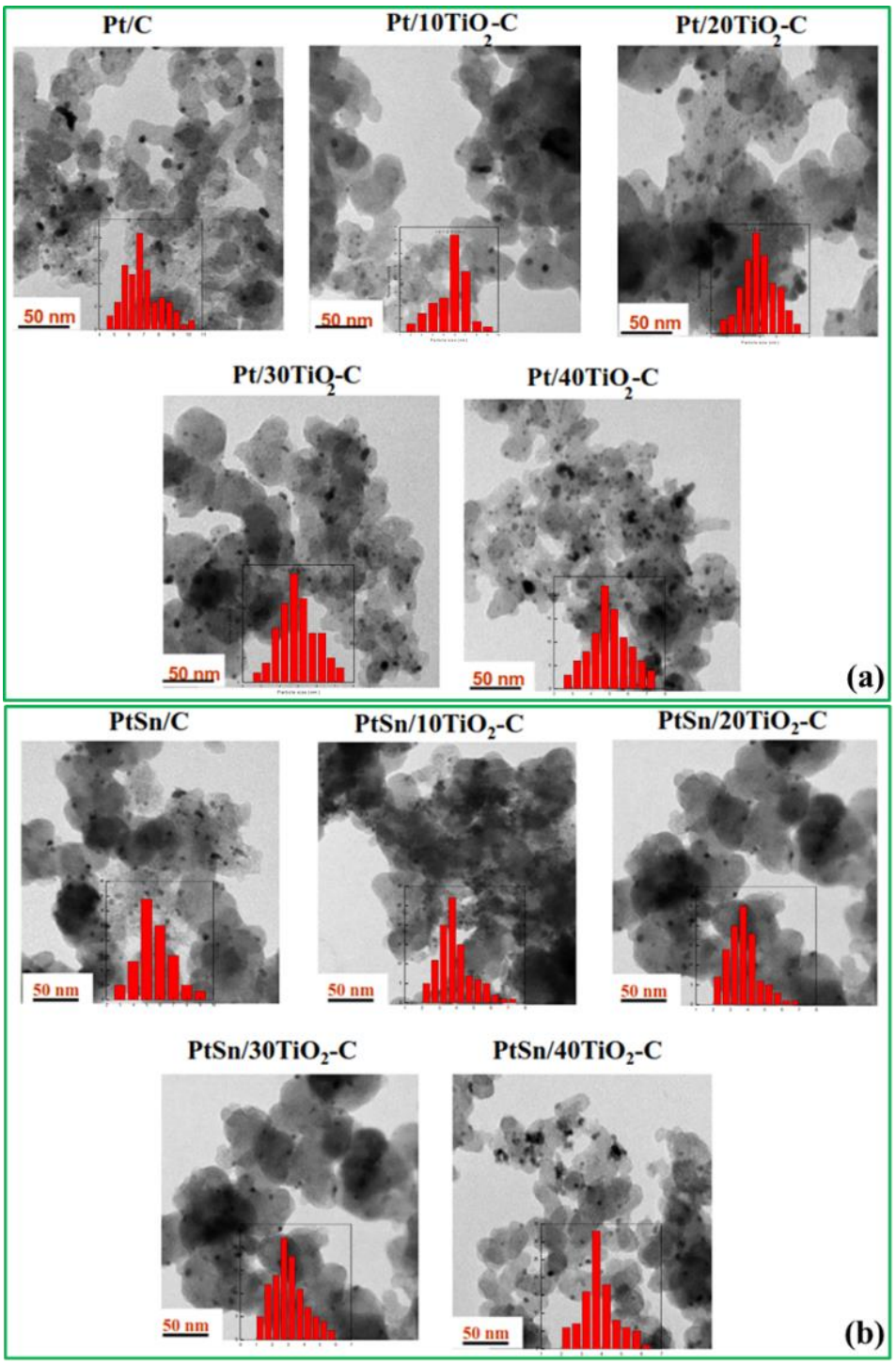

Figure 1. TEM images and their corresponding particle size distribution histograms of (a) Pt/TiO_2-C (b) $PtSn/TiO_2$-C anodic catalysts.

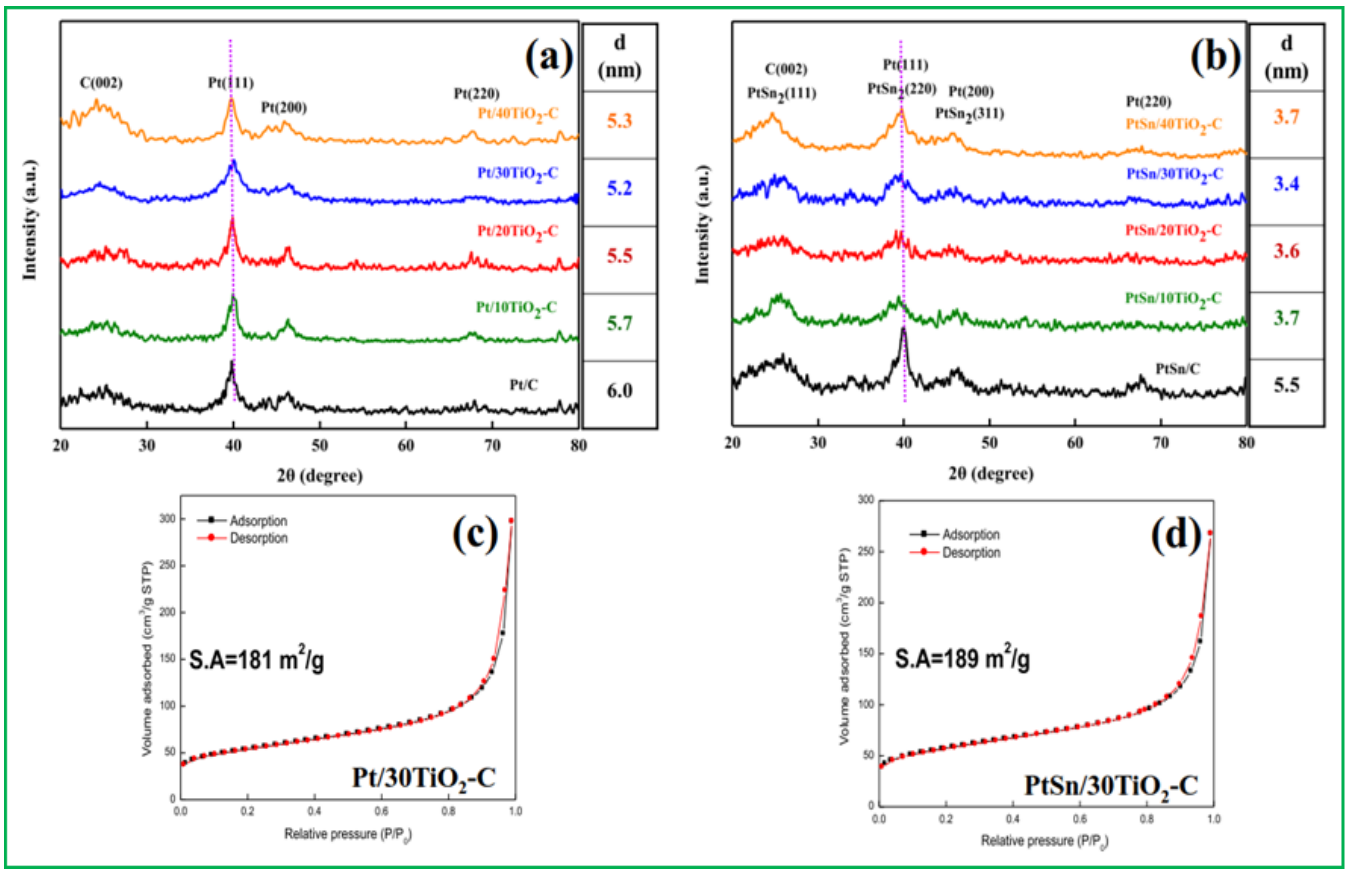

Figure 2. XRD patterns of (a) Pt/TiO_2-C (b) PtSn/TiO_2-C anodic catalysts, N2 adsorption/desorption isotherms of (c) Pt/30TiO_2-C (d) PtSn/30TiO_2-C.

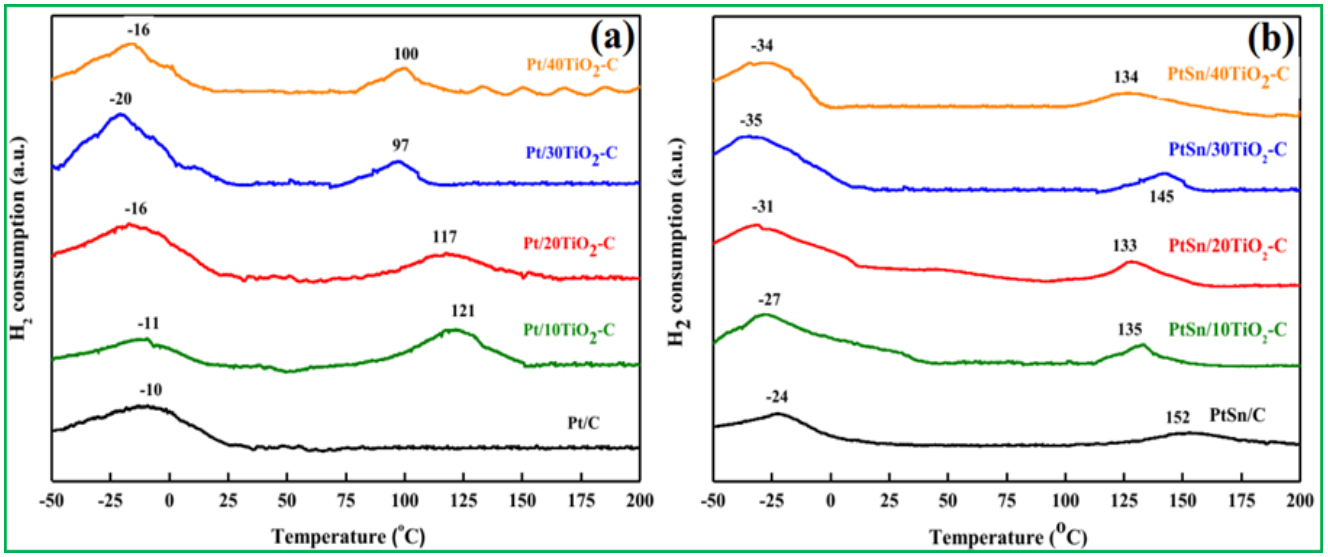

Figure 3. TPR profiles of (a) Pt/TiO_2-C (b) PtSn/TiO_2-C anodic catalysts.

Table 1. Physical and chemical characterization of series Pt/TiO_2-C and PtSn/TiO_2-C anodic catalysts.

Catalyst	TEM d (nm)	Surface area (m^2/g)	EAS (cm^2/mg_{Pt})	TPR	
				T_{r1} (°C)	T_{r2} (°C)
Pt/C	6.9	196	49	-10	---
Pt/10TiO_2-C	5.8	194	152	-11	121
Pt/20TiO_2-C	5.0	184	179	-16	117
Pt/30TiO_2-C	4.8	181	264	-20	97
Pt/40TiO_2-C	4.9	179	229	-16	100
PtSn/C	5.6	221	99	-24	152
PtSn/10TiO_2-C	3.9	210	215	-27	135
PtSn/20TiO_2-C	3.7	193	244	-31	133
PtSn/30TiO_2-C	3.1	189	317	-35	139
PtSn/40TiO_2-C	3.9	178	275	-34	134

Previous literatures [39, 40] reported that in the development of anodic catalysts, via the formation of alloy by adding oxygen-philic metals such as Sn, Ru, Mo, Ti and Os for accelerating the hydrolysis of water was beneficial to provide more surface hydroxyl substance (OH_{ad}). Apparently, based on the measured EAS value, the addition of TiO_2 and Sn enhances the real surface area of platinum, effectively disperses the active species and improves the electro-catalytic activity. If the amount of TiO_2 added too much, the surface Pt will be encased to reduce the surface active sites. The optimal addition of TiO_2 is 30 wt%, which possesses the highest EAS and "intrinsic" activity in the series of catalysts.

3.2 Electrochemical measurements

The maximum current density (Ip) is used to evaluate the activity of alcohols electro-oxidation for anodic catalysts. The first oxidation peak is the current signal of forward potential scanning, which attributes to the oxidation of alcohol; the second oxidation peak is the current signal of reverse potential scanning, which pertains the oxidation of the adsorbed intermediate species, i.e. CO_{ad}. Therefore, we evaluate the activity of alcohols electro-oxidation based on the first oxidation peak. The CV is performed preliminarily on the anodic catalyst through twenty scans of ethanol electro-oxidation to confirm the variability of current density. It shows that the 16^{th} cycle test possesses the highest current density and the best electro-catalytic activity. Therefore, the following evaluation on the activity of alcohols electro-oxidation for series anodic catalysts bases on the data obtained through 16^{th} cycle scans.

In order to understand the function of dopants of TiO_2 and Sn, the series Pt/TiO_2-C and PtSn/TiO_2-C anodic catalysts are executed under same conditions. Figures 4 - 6 manifest the CVs of forward potential scanning for the fabricated anodic catalysts in 1 M MeOH/0.5 M H_2SO_4 (Fig. 4), 1 M

EtOH/0.5 M H_2SO_4 (Fig. 5) and 1 M EG/0.5 M H_2SO_4 (Fig. 6) solution, respectively, with a 50 $mV \cdot s^{-1}$ scanning rate under 25 °C (potential ranges of – 0.2 to 1.0 V vs SCE), and Table 2 notes down the peak current (I_P) and peak potential (E_P) according to the maximum peak current of methanol, ethanol and ethylene glycol electro-oxidation. Brightly, the maximum current density of MOR, EOR and EGOR shows similar and decreases as order of Pt/C < PtSn/C < Pt/TiO_2-C < PtSn/TiO_2-C, Pt/10TiO_2-C < Pt/20TiO_2-C < Pt/40TiO_2-C < Pt/30TiO_2-C, and PtSn/10TiO_2-C < PtSn/20TiO_2-C < PtSn/40TiO_2-C < PtSn/30TiO_2-C, respectively. The magnitude of current density on the forward potential scanning displays the electro-catalytic activity of alcohol oxidation. The order is constant with the measured EAS, surface area and particle size of catalysts. The dopants of TiO_2 and Sn upgrade the EAS and surface area, and lower the particle size of platinum of anodic catalysts, as well as possessing higher electro-catalytic activity. Also, the optimal addition of TiO_2 can preserve against the agglutination of active species during the alcohol oxidation, and exhibits an efficiency performance on the alcohols electro-oxidation. Both the PtSn/30TiO_2-C and Pt/30TiO_2-C anodic catalysts indicate higher dispersion among these series anodic catalysts. Previous literatures [41-43] reported that the decoration of Pt catalyst by TiO_2 and Sn emerged multiple available surface oxide, i.e., OH_{ad} sites, which enhanced the electro-catalytic activity. Obviously, the active species can be well-dispersed effectively by the addition of Sn and TiO_2, and facilitates the oxidation of alcohols and adsorbed intermediates with the surface OH_{ad} sites. Therefore, the function of the TiO_2 and Sn dopants can produce more oxygen-containing functional groups, provides more active sites, increases the active surface area, and then enhances the electro-catalytic activity of anodic catalysts.

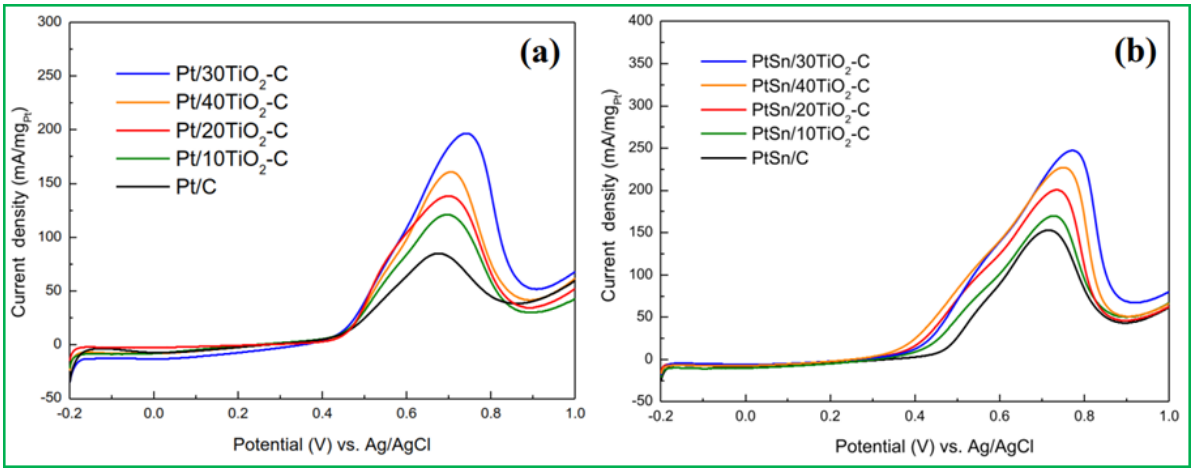

Figure 4. CV curves of (a) Pt/TiO_2-C (b) PtSn/TiO_2-C electrodes in 1 M MeOH/0.5 M H_2SO_4 solution with a scan rate of 50 $mV \cdot s^{-1}$ at 25 °C.

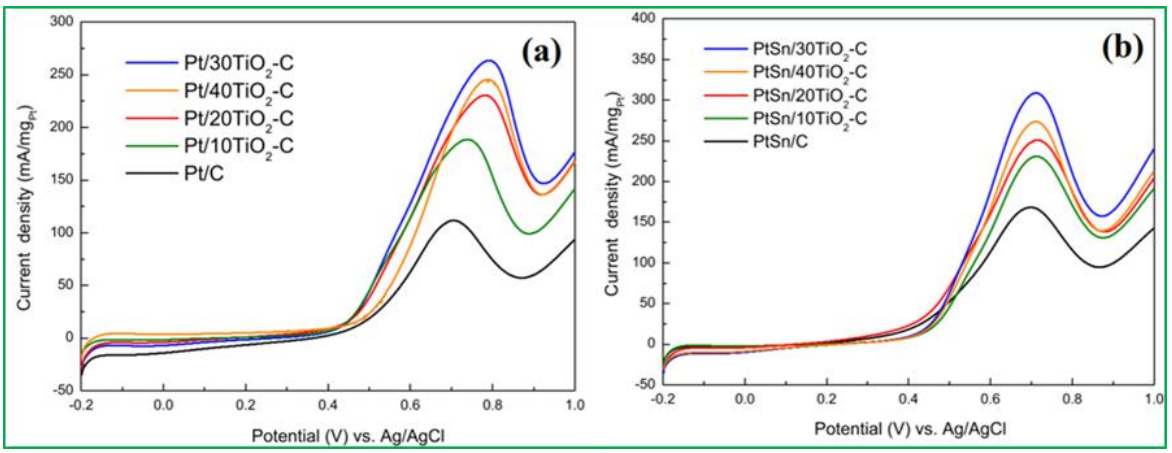

Figure 5. CV curves of (a) Pt/TiO_2-C (b) $PtSn/TiO_2$-C electrodes in 1 M EtOH/0.5 M H_2SO_4 solution with a scan rate of 50 $mV \cdot s^{-1}$ at 25 °C.

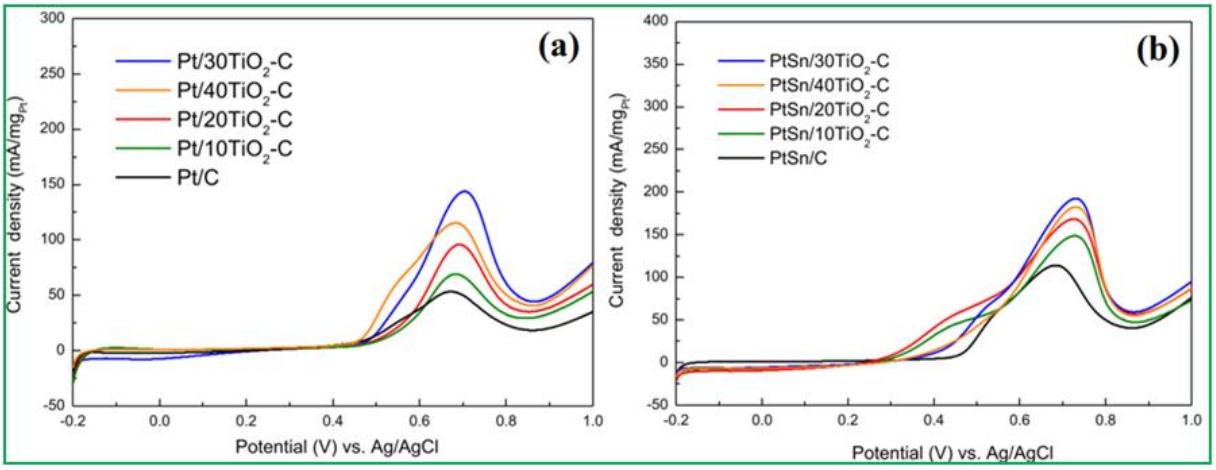

Figure 6. CV curves of (a) Pt/TiO_2-C (b) $PtSn/TiO_2$-C electrodes in 1 M EG/0.5 M H_2SO_4 solution with a scan rate of 50 $mV \cdot s^{-1}$ at 25 °C.

Table 2. Performance of MOR, EOR and EGOR over Pt/TiO_2-C and $PtSn/TiO_2$-C anodic catalysts.

Catalyst	MOR		EOR		EGOR	
	I_P (mA/mg_{Pt})	E_P (V)	I_P (mA/mg_{Pt})	E_P (V)	I_P (mA/mg_{Pt})	E_P (V)
Pt/C	85	0.68	111	0.70	53	0.67
$Pt/10TiO_2$-C	121	0.70	189	0.74	69	0.68
$Pt/20TiO_2$-C	138	0.70	230	0.78	96	0.69
$Pt/30TiO_2$-C	197	0.74	263	0.79	144	0.70
$Pt/40TiO_2$-C	160	0.71	245	0.79	115	0.68
PtSn/C	153	0.71	168	0.70	113	0.69
$PtSn/10TiO_2$-C	169	0.72	231	0.71	148	0.71
$PtSn/20TiO_2$-C	200	0.73	251	0.72	168	0.71
$PtSn/30TiO_2$-C	247	0.75	310	0.71	192	0.72
$PtSn/40TiO_2$-C	227	0.78	274	0.71	182	0.72

Figure 7 emerges the variations of Pt/C, Pt/30TiO_2-C and PtSn/30TiO_2-C anodic catalysts with MOR, EOR and EGOR. It affirmes that the current density elevates 132%, 138% and 172%, respectively for the MOR, EOR and EGOR as doping the TiO_2, and promotes 25%, 17% and 33%, respectively for the MOR, EOR and EGOR as doping the Sn. On the whole, in the electro-oxidation reaction of alcohols, the activity of simultaneous addition of TiO_2 and Sn at the same time is higher than that of adding only TiO_2, and it is better than adding none. The PtSn/30TiO_2-C is a more apposite electro-catalyst, which possesses better performance. The electro-catalytic activity of alcohols for the three catalysts follows the order of PtSn/30TiO_2-C > Pt/30TiO_2-C > Pt/C, and according to the discrepancy of the current density, the electro-catalytic activity of alcohols for any one of the catalysts follows the order of EOR > MOR > EGOR. Such tendency can be related with the amount of CO formed in each oxidation reaction; the CO_{ad} (adsorbed CO) is the major poisoning specie in the MOR, while CH_3CHO and CH_3COOH [44] prevail over the CO_{ad} as the principal products in the EOR. Also, series anodic catalysts were more active for the EOR and MOR because other reaction intermediates, $C_2H_4O_3$ and $C_2H_2O_4$, [45] and diverse products may be adsorbed during the EGOR besides CO_{ad} causes poisoning of catalysts, and consequently decreasing the electro-oxidation activity.

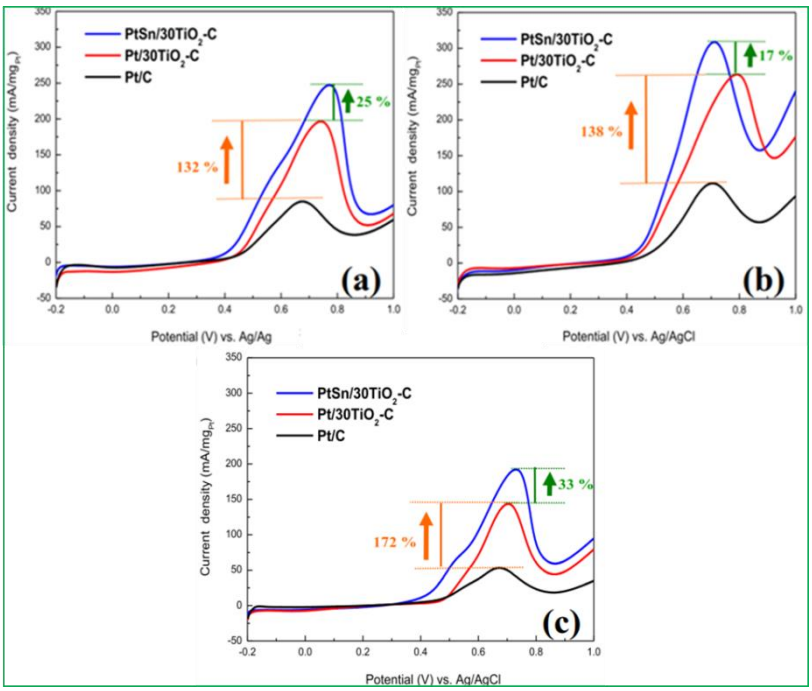

Figure 7. CV curves of Pt/C, Pt/30TiO_2-C and PtSn/30TiO_2-C electrodes in (a) 1 M MeOH/0.5 M H_2SO_4 (b) 1 M EtOH/0.5 M H_2SO_4 (c) 1 M EG/0.5 M H_2SO_4.

In order to assess the electrochemical durability of alcohols electro-oxidation in an acidic medium, the chronoamperometric test has been carried out further to judge the stability of MOR, EOR and EGOR. Three selected Pt/C, Pt/30TiO_2-C and PtSn/30TiO_2-C anodic catalysts retain under a fixed voltage (0.45 V) for a long time (3600 s) scanning in 1 M MeOH/0.5 M H_2SO_4, 1 M EtOH/0.5 M H_2SO_4 and 1 M EG/0.5 M H_2SO_4 solution, respectively. Figure 8 and Figure 9 emerge the variations of amperometric *I-t* curves for the MOR, EOR and EGOR with the three anodic catalysts. It indicates that

the current density of the three catalysts decays rapidly in the initial few minutes, and then keeps a steady current density. The declination of current density is due to the adsorbed intermediate species via the oxidation of alcohol, i.e., CO_{ad} on the surface which inhibits the alcohol further oxidation, and the rate of declination relies on the strength of CO_{ad} [46]. Obviously, the trend indicates that the current densities of the three alcohols are less than 10 mA/mg_{Pt}, 30 ~ 45 mA/mg_{Pt} and 40 ~ 60 mA/mg_{Pt}, respectively, for the Pt/C, Pt/30TiO_2-C and PtSn/30TiO_2-C anodic catalysts after scanning of 3600 s. Previous literatures [47, 48] reported that the stable current was proportional to the electro-catalytic activity, and the larger the stable current possessed the better performance. Therefore, addition of TiO_2 only or simultaneous addition of TiO_2 and Sn to modify the Pt/C catalyst improves the electro-catalytic activity and enhances the stability of the anodic catalyst.

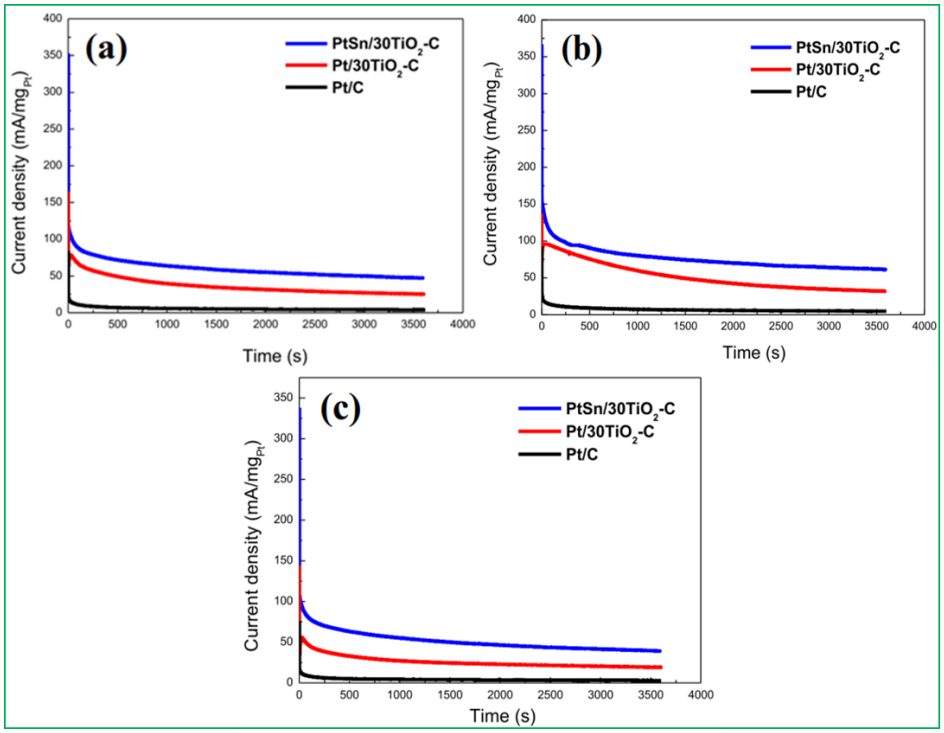

Figure 8. Current density-time curves at 0.45 V for scanning 3600 s for the selected Pt/C, Pt/30TiO_2-C and PtSn/30TiO_2-C electrodes in (a) 1 M MeOH/0.5 M H_2SO_4 (b) 1 M EtOH/0.5 M H_2SO_4 (c) 1 M EG/0.5 M H_2SO_4.

The PtSn/30TiO_2-C exhibits a more appropriate electro-catalyst, which possesses better performance and stability. The durability of alcohols electro-oxidation of the three catalysts follows the order of PtSn/30TiO_2-C > Pt/30TiO_2-C > Pt/C, and in accordance with the decay of current density, the electrochemical durability of alcohols for any one of the catalysts follows the order of EOR > MOR > EGOR.

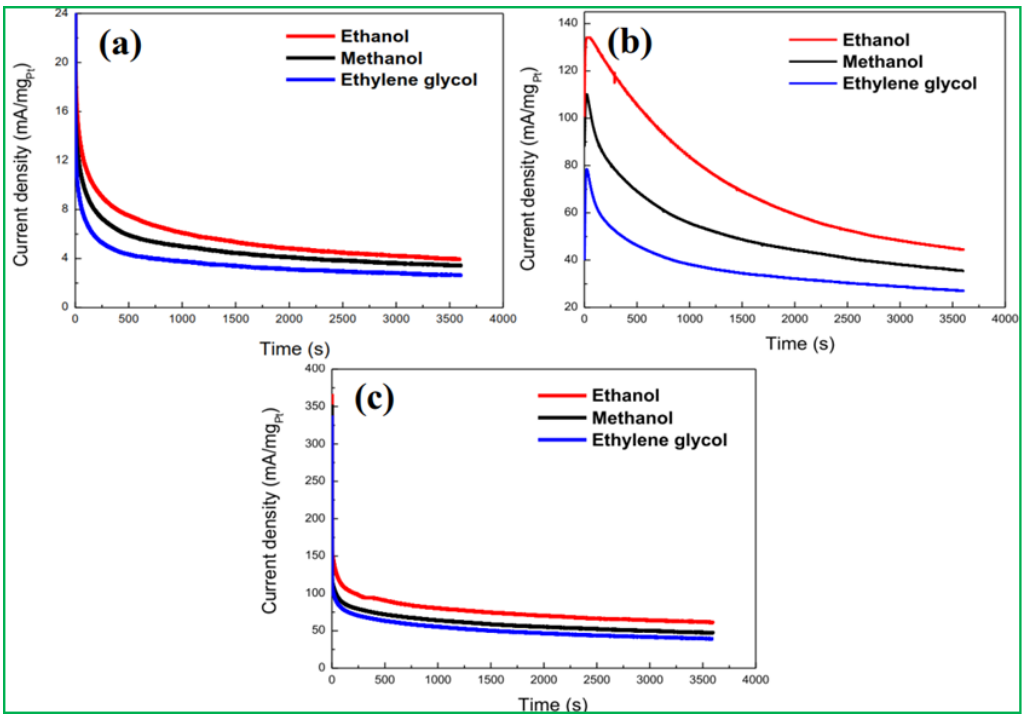

Figure 9. Current density-time curves at 0.45 V for scanning 3600 s in alcohols solution for the selected (a) Pt/C (b) Pt/30TiO_2-C (c) PtSn/30TiO_2-C electrodes.

4. CONCLUSIONS

In the present work, series Pt/TiO_2-C and PtSn/TiO_2-C anodic catalysts have been fabricated and evaluated the electro-oxidation of alcohols, which can be premeditated as a candidate in the using of direct alcohol fuel cells in coming times. The results of this study revealed that the role of doped TiO_2 and Sn produced more oxygen-containing functional groups, provided more active sites and increased the active surface area. Simultaneous addition of TiO_2 and Sn to modify the Pt/C catalyst upgraded the EAS and surface area, and lowered the particle size of platinum of anodic catalysts, as well as enhanced the electro-catalytic activity. The PtSn/30TiO_2-C catalyst exhibited the preferential electro-catalytic activity and stability among the fabricated series anodic catalysts. The electro-catalytic activity and durability of alcohols for any one of the catalysts followed the order of EOR > MOR > EGOR

ACKNOWLEDGEMENT
We are pleased to acknowledge the financial support for this study from the Ministry of Science and Technology of the Republic of China under contract numbers of MOST 107-2113-M-606-001- and MOST 108-2113-M-606-001-.

References

1. M.A. Abdelkareem, E.T. Sayed, H.O. Mohamed, M. Obaid, H. Rezk, K.J. Chae, *Prog. Energy Combust. Sci.,* 77 (2020) 52.
2. L. Feng, H. Xue, *ChemElectroChem.,* 4 (2017) 20.

3. J. Chang, L. Feng, K. Jiang, H. Xue, W.B. Cai, C. Liu, W. Xing, *J. Mater. Chem. A,* 4 (2016) 18607.
4. C. Bianchini, P.K. Shen, *Chem. Rev.,* 109 2009) 4183.
5. H. Yue, Y. Zhao, X. Ma, J. Gong, *Chem. Soc. Rev.,* 41 (2012) 4218.
6. Y. Wang, S. Zou, W.B. Cai, *Catalysts,* 5 (2015) 1507.
7. B. Fang, L. Feng, *Acta Phys. Chim. Sin.,* 36 (2020) 1905023.
8. S. Chen, H. Xu, B. Yan, S. Li, J. Dai, C. Wang, Y. Shiraishi, Y. Du, *J. Taiwan Inst. Chem. Eng.,* 83(2018) 64.
9. Y. Xu, B. Zhang, *Chem. Soc. Rev.,* 43 (2014) 2439.
10. S. Xing, Z. Liu, Q. Xue, S. Yin, F. Li, W. Cai, S. Li, P. Chen, P. Jin, H. Yao, Y. Chen, *Appl. Catal. B,* 259 (2019) 118082.
11. Y.X. Chen, A. Lavacchi, H.A. Miller, M. Bevilacqua, J. Filippi, M. Innocenti, A. Marchionni, W. Oberhauser, L. Wang, F. Vizza, *Nat. Commun.,* 5 (2014) 4036.
12. J. Zheng, D.A. Cullen, R.V. Forest, J.A. Wittkopf, Z. Zhuang, W. Sheng, J.G. Chen, Y. Yan, *ACS Catal.,* 5 (2015) 1468.
13. X. Yue, Y. Pu, W. Zhang, T. Zhang, W. Gao, *J. Energ. Chem.,* 49 (2020) 275.
14. F.C. Simoes, D.M. dos Anjos, F. Vigier, J.M. Ĺeger, F. Hahna, C. Coutanceau, E.R. Gonzalez, G. Tremiliosi-Filho, A.R. de Andrade, P. Olivi, K.B. Kokoh, *J. Power Sources,* 167 (2007) 1.
15. H. Liu, D. Yang, Y. Bao, X. Yu, L. Feng, *J. Power Sources,* 434 (2019) 226754.
16. C. Chen, H. Xu, H. Shang, L. Jin, T. Song, C. Wang, F. Gao, Y. Zhang, Y. Du, *Nanoscale,* 11 (2019) 20090.
17. W. Chen, J. Xue, Y. Bao, L. Feng, *Chem. Eng. J.,* 381 (2020) 122752.
18. Q. Wang, S. Chen, J. Jiang, J. Liu, J. Deng, X. Ping, Z. Wei, *Chem. Commun. (Camb),* 56 (2020) 2419.
19. X. Zhou, Y. Gan, J. Du, D. Tian, R. Zhang, C. Yang, Z. Dai, *J. Power Sources,* 232 (2013) 310.
20. N. Pongpichayakul, P. Waenkeaw, J. Jakmunee, S. Themsirimongkon, S. Saipanya, *J. Appl. Electrochem.,* 50 (2019) 51.
21. Y. Duan, Y. Sun, L. Wang, Y. Dai, B. Chen, S. Pan, J. Zou, *J. Mater. Chem. A,* 4 (2016) 7674.
22. F. Wang, H. Yu, Z. Tian, H. Xue, L. Feng, *J. Energ. Chem.,* 27 (2018) 395.
23. C. Feng, T. Takeuchi, M.A. Abdelkareem, T. Tsujiguchi, N. Nakagawa, *J. Power Sources,* 242 (2013) 57.
24. J. Liu, J. Ye, C. Xu, S. Jiang, Y. Tong, *Electrochem. Comm.,* 9 (2007) 2334.
25. M. Javier, H. Dirk, L.M. Marıa-Jose, S. Volker, B. Detlef, *Appl. Catal. B,* 62 (2006) 201.
26. E.H. Brian, V.M. Dzmitry, P. Derek, *Electrochem. Commun.,* 3 (2001) 395.
27. C.H. Liu, M.H. Liu, Y.H. Liu, C.J. Lu, C.C. Chang, C.C. Wang, C.B. Wang, Int. J. Electrochem. Sci., 15 (2020) 12395.
28. C. Moitrayee, C. Abhik, G. Susanta, I. Basumallick, *Electrochimica Acta,* 54 (2009) 7299.
29. A. Pozio, M. De Francesco, A. Cemmi, F. Cardellini, L. Giorgi, *J. Power Sources,* 105 (2002) 13.
30. G. Faubert, D. Guay, J.P. Dodelet, *J. Electrochem. Soc.,* 145 (1998) 2985.
31. K. Woods, *J. Electrochem. Soc.,* 9 (1976) 1.
32. C.B. Zhang, H. He, K.I. Tanaka, *Appl. Catal. B,* 65 (2006) 37.
33. W. Zhou, Z. Zhou, S. Song, W. Li, G. Sun, P. Tsiakaras, Q. Xin, *Appl. Catal. B,* 46 (2003) 273.
34. J. Llorca, N. Homs, J.L.G. Fierro, J. Sales, P.R. de la Piscina, *J. Catal.,* 166 (1997) 44.
35. V. Grolier, R. Schmid-Fetzer, *J. Alloys Compd.,* 450 (2008) 264.
36. A.E. Alvarez, A.N. Gravina, J.M. Sieben, P.V. Messina, M.M.E. Duarte, *Mater. Sci. Eng. B,* 211 (2016) 26.
37. H. Armendáriz, A. Guzmán, J.A. Toledo, M.E. Llanos, A. Vázquez, G. Aguilar-Ríos, *Appl. Catal. A,* 211 (2001) 69.
38. A.D. Ballarini, S.R. de Miguel, A.A. Castro, O.A. Scelza, *Appl. Catal. A,* 467 (2013) 235.
39. E. Antolini, F. Colmati, E.R. Gonza´ lez, *Electrochem. Commun.,* 9 (2007) 398.

40. M. Barroso de Oliveira, L.P.R. Profeti, P. Olivi, *Electrochem. Commun.,* 7 (2005) 703.
41. E. Antolini, F. Colmati, E.R. Gonza´ lez, *Electrochem. Commun.,* 9 (2007) 398.
42. M. Barroso de Oliveira, L.P.R. Profeti, P. Olivi, *Electrochem. Commun.,* 7 (2005) 703.
43. J. Mann, N. Yao, Andrew B. Bocarsly, *Langmuir,* 22 (2006) 10432.
44. T. Iwasita, Methanol and CO electrooxidation. John Wiley & Sons, Ltd., (2003).
45. H. Wang, Z. Jusys, R.J. Behm, *J. Power Sources,* 154 (2006) 351.
46. X. He, C. Hu, *J. Power Sources,* 196 (2011) 3119.
47. H. Song, X. Qiu, X. Li, F. Li, W. Zhu, L. Cuen, *J. Power Sources,* 170 (2007) 50.
48. Y.H. Qina, H.C. Li, H.H. Yanga, X.S. Zhanga, X.G. Zhoua, N. Li, W.K. Yuana, *J. Power Sources,* 196 (2011) 159.